

Monothioether Complexes of Osmium: The *trans*-[OsBr₄(SR₂)₂] Family and *mer*-[OsBr₃(SR₂)₃] Precursors

Kausikisankar Pramanik, Prasanta Ghosh, and Animesh Chakravorty*

Department of Inorganic Chemistry, Indian Association for the Cultivation of Science, Calcutta 700 032, India

Received February 6, 1998

Introduction

Simple monothioethers (R₂S, R = alkyl) have long been known to have good affinity for platinum metal ions. Two of the well-documented types of complexes are [M^{III}X₃(SR₂)₃] (M = Ru, Rh, Ir; X⁻ = halide) and [M^{IV}X₄(SR₂)₂] (M = Ir, Pt).^{1–5} In the case of osmium, just one compound of the former type (but none of the latter type) is known.⁶ The difficulty lies in the lack of availability of convenient synthetic methods. For example, the reaction of R₂S with [OsX₆]²⁻ salts failed to afford tractable thioether complexes.⁷

A synthesis of *mer*-[OsBr₃(SR₂)₃] via deoxygenation of R₂-SO by [OsBr₆]²⁻ was recently developed in this laboratory.⁸ The trivalent complexes have now provided facile access to the hitherto unknown [OsBr₄(SR₂)₂] family. The X-ray structures of two of these are reported along with that of a *mer*-[OsBr₃(SR₂)₃] precursor. This has provided an opportunity for assessing the valence dependence of Os–SR₂ back-bonding. Metal reduction potentials are strongly dependent on the Br⁻:R₂S ratio.

Results and Discussion

A. Synthesis and Characterization. The dark colored [Os^{IV}Br₄(SR₂)₂] complexes **1a–c** having *trans* geometry (vide infra; Chart 1) are furnished in good yield by the reaction of *mer*-[Os^{III}Br₃(SR₂)₃],⁸ **2a–c**, with excess bromine in benzene

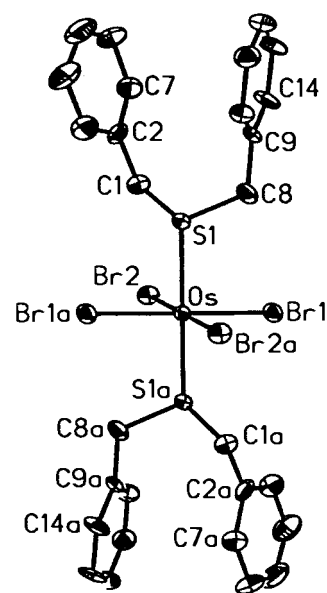


Figure 1. ORTEP plot and atom-labeling scheme for *trans*-[OsBr₄{S(CH₂Ph)₂}₂] (**1b**). All non-hydrogen atoms are represented by their 30% probability ellipsoids.

Chart 1



solution at room temperature. There is no indication that the *cis* isomer of **1** is formed in this reaction. To our knowledge **1a–c** represent the first examples of osmium(IV) complexes of monodentate thioethers. A few osmium(IV) species incorporating bi/polythioethers chelation are known but none of these have been structurally characterized.^{4b,7}

Spectral and magnetic characterization data of the complexes are listed in the Experimental Section. The type **1** species display intense absorption near 500 nm presumably due to Br⁻/S⁻→Os^{IV} charge transfer.^{1d,6} Significantly, in the less oxidized type **2** species, the band system lies at higher energy, ~450 nm. The magnetic moments (~1.7 μ_B) of type **1** complexes are low evidently due to high spin–orbit coupling.⁹

B. Structure. The X-ray structures of **1b** and **1c** have been determined revealing centrosymmetric *trans* geometry. Molecular views are shown in Figures 1 and 2, and selected bond parameters are listed in Table 1. The S–Os–S axis is tilted with respect to the normal to the OsBr₄ plane, the tilt angle being 8.4 and 5.7°, respectively for **1b** and **1c**.

- (1) (a) Jaswal, J. S.; Retting, S. J.; James, B. R. *Can. J. Chem.* **1990**, *68*, 1808. (b) Yapp, D. T. T.; Jaswal, J. S.; Retting, S. J.; James, B. R.; Skov, K. A. *Inorg. Chim. Acta* **1990**, *177*, 199. (c) Sarma, U. C.; Sarma, K. P.; Poddar, P. K. *Polyhedron* **1988**, *7*, 1737. (d) Fergusson, J. E.; Karran, J. D.; Seevaratnam, S. *J. Chem. Soc.* **1965**, 2627.
- (2) (a) Allen, E. A.; Wilkinson, W. *J. Chem. Soc., Dalton Trans.* **1972**, 613. (b) Anderson, S. J.; Barnes, J. R.; Goggin, P. L.; Goodfellow, R. *J. J. Chem. Res. (M)* **1978**, 3601. (c) Kukushkin, Yu. N.; Rubtsova, N. D.; Ivannikova, N. V. *Zh. Neorg. Khim.* **1970**, *15*, 1328. (d) Fritzmman, E. K.; Krinitskii, V. V. *J. Appl. Chem. (U.S.S.R.)* **1938**, *11*, 1610.
- (3) (a) Kauffman, G. B.; Tsai, J. H.-S.; Gubelmann, M. H.; Williams, A. F. *J. Chem. Soc., Dalton Trans.* **1980**, 1791. (b) Kauffman, G. B.; Tsai, J. H.-S.; Fay, R. C.; Jørgensen, C. K. *Inorg. Chem.* **1963**, *2*, 1233. (c) Rây, P. C.; Adhikari, N.; Ghosh, R. *J. Indian Chem. Soc.* **1933**, *10*, 275.
- (4) (a) Cipriano, R. A.; Levason, W.; Pletcher, D.; Powell, N. A.; Webster, M. *J. Chem. Soc., Dalton Trans.* **1987**, 1901. (b) Gulliver, D. J.; Levason, W.; Smith, K. G.; Selwood, M. J.; Murray, S. G. *J. Chem. Soc., Dalton Trans.* **1980**, 1872.
- (5) (a) Kukushkin, V. Yu. *Coord. Chem. Rev.* **1995**, *139*, 375 and references therein. (b) Goggin, P. L.; Goodfellow, R. J.; Haddock, S. R.; Knight, J. R.; Reed, F. J. S.; Taylor, B. F. *J. Chem. Soc., Dalton Trans.* **1974**, 523. (c) Kauffman, G. B.; Tsai, J. H.-S.; Takahashi, L. T. *Inorg. Synth.* **1966**, *8*, 245.
- (6) Aires, B. E.; Fergusson, J. E.; Howarth, D. T.; Miller, J. M. *J. Chem. Soc. A* **1971**, 1144.
- (7) Ali, R.; Higgins, S. J.; Levason, W. *Inorg. Chim. Acta* **1984**, *84*, 65.
- (8) Ghosh, P.; Pramanik, K.; Chakravorty, A. *J. Chem. Soc., Chem. Commun.* **1995**, 477.

- (9) (a) Figgis, B. N.; Lewis, J. *Prog. Inorg. Chem.* **1964**, *6*, 165. (b) Chatt, J.; Leigh, G. J.; Mingos, D. M. P.; Paske, R. J. *J. Chem. Soc. A* **1968**, 2636.

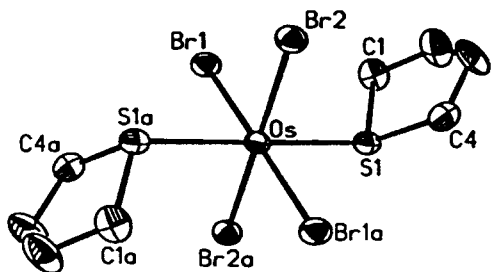


Figure 2. ORTEP plot and atom-labeling scheme for *trans*-[OsBr₄{S(CH₂)₄}₂] (**1c**). All non-hydrogen atoms are represented by their 30% probability ellipsoids.

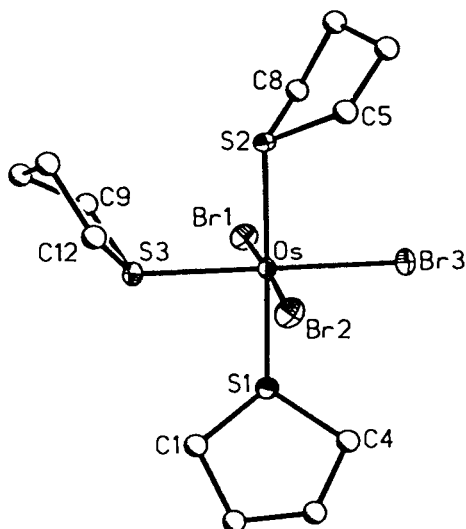


Figure 3. Perspective view and atom-labeling scheme for *mer*-[OsBr₃{S(CH₂)₄}₃] (**2c**).

Table 1. Selected Bond Lengths (Å) and Angles (°) for **1b** and **1c**

	1b	1c
Os–Br1	2.472(2)	2.468(3)
Os–Br2	2.441(2)	2.455(3)
Os–S1	2.420(4)	2.401(7)
Br1–Os–Br2	90.3(1)	89.6(1)
Br1–Os–S1	96.6(1)	94.8(2)
Br2–Os–S1	95.1(1)	93.0(2)

Table 2. Selected Bond Lengths (Å) and Angles (°) for **2c**

Os–Br1	2.494(2)	Os–Br2	2.494(2)
Os–Br3	2.518(3)	Os–S1	2.383(5)
Os–S2	2.380(5)	Os–S3	2.382(6)
Br1–Os–Br2	176.7(1)	Br1–Os–Br3	90.5(1)
Br2–Os–Br3	91.4(1)	Br1–Os–S1	86.6(1)
Br2–Os–S1	90.7(1)	Br3–Os–S1	90.0(1)
Br1–Os–S2	91.8(1)	Br2–Os–S2	90.9(1)
Br3–Os–S2	91.0(1)	S1–Os–S2	178.1(2)
Br1–Os–S3	88.4(1)	Br2–Os–S3	89.7(1)
Br3–Os–S3	178.9(1)	S1–Os–S3	89.9(2)
S2–Os–S3	89.1(2)		

The X-ray structure of **2b** was reported earlier (Os–Br, 2.495(2) and 2.497(2) Å, and Os–S, 2.398(3) and 2.387(5) Å).⁸ That of **2c** has now been determined (Figure 3 and Table 2). The data permits comparisons within the **1b**–**2b** and **1c**–**2c** pairs.

In each pair the Os–Br length follows the order **1** < **2**. This is consistent with the electrostatic effect of the greater charge on the tetravalent atom in **1**. The implication is that the Os–Br bond is primarily σ in character. The reversed order (**1** > **2**) of Os–S length is attributed to $5d\pi(\text{Os}) \rightarrow 3d\pi(\text{S})$ back-

Table 3. Electrochemical Data^a

compound	$E_{1/2}, \text{V} (\Delta E_p, ^b \text{ mV})$		compound	$E_{1/2}, \text{V} (\Delta E_p, ^b \text{ mV})$	
	$\text{Os}^{\text{IV}}/\text{Os}^{\text{III}}$			$\text{Os}^{\text{IV}}/\text{Os}^{\text{III}}$	
1a	0.45	(120)	2a^c	1.00	(110)
1b	0.47	(110)	2b^c	1.07	(130)
1c	0.42	(110)	2c^c	0.96	(140)

^a In 5:1 dichloromethane–acetonitrile mixture at 298 K. ^b ΔE_p = peak-to-peak separation. ^c $\text{Os}^{\text{III}}/\text{Os}^{\text{II}}$ $E_{1/2}$ [V] (ΔE_p [mV]) values: **2a**, –0.46 (110); **2b**, –0.33 (130); **2c**, –0.50 (140).

bonding ($\text{Os}^{\text{III}} \gg \text{Os}^{\text{IV}}$). The back-bonding ability of Os^{III} has been documented.¹⁰

C. Metal Redox: Valence Stability vis-à-vis $\text{Br}^-:\text{R}_2\text{S}$ Ratio. Both **1** and **2** are electroactive and display quasireversible cyclic voltammograms in solution. Reduction potential data are listed in Table 3. The osmium(IV)–osmium(III) couple shifts dramatically from ~0.4 to ~1.0V vs SCE as the $\text{Br}^-:\text{R}_2\text{S}$ ratio changes from 4:2 (**1**) to 3:3 (**2**). The net result is that under ambient conditions the Br_4S_2 and Br_3S_3 spheres respectively stabilize the tetravalent and the trivalent states of the metal. For type **2** complexes the osmium(III)–osmium(II) couple is also observed (~–0.4 V). The electrogenerated $[\text{Os}^{\text{III}}\text{Br}_4(\text{SR}_2)_2]^-$ and $[\text{Os}^{\text{IV}}\text{Br}_3(\text{SR}_2)_3]^+$ species are unstable and could not be isolated.

Concluding Remarks

The main findings of the present work are as follows. The first family of $[\text{Os}^{\text{IV}}\text{X}_4(\text{SR}_2)_2]$ complexes incorporating monothioethers and having centrosymmetric *trans* geometry has been synthesized in good yield in the case of X = Br via oxidative bromination of *mer*- $[\text{Os}^{\text{III}}\text{Br}_3(\text{SR}_2)_3]$. In this transformation the osmium(IV)–osmium(III) reduction potential is lowered by a remarkable ~0.6 V. The bond length trend ($\text{Os}^{\text{IV}}\text{–Br} < \text{Os}^{\text{III}}\text{–Br}$; $\text{Os}^{\text{IV}}\text{–S} > \text{Os}^{\text{III}}\text{–S}$) among *trans*- $[\text{OsBr}_4(\text{SR}_2)_2]$ and *mer*- $[\text{OsBr}_3(\text{SR}_2)_3]$ is indicative of relatively poor $\text{Os}^{\text{IV}}\text{–SR}_2$ back-bonding in the former complexes.

Experimental Section

Materials. The compound $(\text{NH}_4)_2[\text{OsBr}_6]$ was prepared from $[\text{OsO}_4]$ (Arora-Mathey, India) by a reported procedure.¹¹ Electrochemical grade dichloromethane, acetonitrile, and tetraethylammonium perchlorate (TEAP) were obtained as before.¹² All other chemicals and solvents were of analytical grade. Dimethyl sulfoxide (Merck, India), dibenzyl sulfoxide (Fluka, Switzerland) and tetramethylene sulfoxide (Aldrich, USA) were used.

Physical Measurements. A Hitachi 330 spectrophotometer was used to record UV/visible/near-IR spectra. The EPR spectra were obtained at X-band frequencies with a Varian E-109C spectrometer fitted with a quartz Dewar. The calibrant was DPPH ($g = 2.0037$). Room-temperature magnetic susceptibilities were measured with a model 155 PAR vibrating-sample magnetometer fitted with a Walker Scientific L75FBAL magnet. A Perkin-Elmer 240C elemental analyzer was used to collect microanalytical data (C, H). All electrochemical measurements were performed under nitrogen atmosphere using a PAR 370-4 electrochemistry system as before:^{12b} working electrode, platinum disk; reference electrode, saturated calomel electrode (SCE); auxiliary electrode, platinum wire; supporting electrolyte, NEt_4ClO_4 (0.1 M); scan rate, 50 mV s^{-1} ; solute concentration 10^{-3} M. All potential reported in this work are uncorrected for junction contribution.

(10) (a) Taube, H. *Pure Appl. Chem.* **1979**, *51*, 901. (b) Sekine, M.; Harman, W. D.; Taube, H. *Inorg. Chem.* **1988**, *27*, 3604.

(11) Dwyer, F. P.; Hogarth, J. W. *Inorg. Synth.* **1957**, *5*, 204.

(12) (a) Lahiri, G. K.; Bhattacharya, S.; Ghosh, B. K.; Chakravorty, A. *Inorg. Chem.* **1987**, *26*, 4324. (b) Chandra, S. K.; Basu, P.; Ray, D.; Pal, S.; Chakravorty, A. *Inorg. Chem.* **1990**, *29*, 2423.

Preparation of Complexes. *trans*-[OsBr₄(SMe₂)₂] (**1a**). To a solution of *mer*-[OsBr₃(SMe₂)₃] (60 mg, 0.095 mmol) in 40 mL of benzene bromine (~0.05 mL, 1.0 mmol) was added and magnetically stirred. After 24 h another ~0.05 mL of bromine was added and stirring was continued for another 24 h. The color changed from orange to deep red. After removing the volatiles under reduced pressure the mixture was kept in vacuo overnight. Upon chromatographic purification of the residue on neutral silica gel with 1:2 hexane/benzene mixture as eluent, *trans*-[OsBr₄(SMe₂)₂] was obtained. Yield 70%. Anal. Calcd for C₂₄H₁₂S₂Br₄Os: C, 7.58; H, 1.91. Found: C, 7.5; H, 2.0. μ_{eff} (solid, 298 K): 1.73 μ_{B} . Spectral data: UV/visible/near-IR in CH₂Cl₂ (λ_{max} , nm (ϵ , M⁻¹ cm⁻¹)), 503 (7600), 538 (7250), 676 (390), 835 (43), 1820 (82).

trans-[OsBr₄{S(CH₂Ph)₂}]₂ (**1b**). This was prepared by the above procedure using *mer*-[OsBr₃{S(CH₂Ph)₂}]₃ as precursor complex. Yield 70%. Anal. Calcd for C₂₈H₂₈S₂Br₄Os: C, 35.83; H, 3.01. Found: C, 36.1; H, 2.9. μ_{eff} (solid, 298 K): 1.74 μ_{B} . Spectral data: UV/visible/near-IR in CH₂Cl₂ (λ_{max} , nm (ϵ , M⁻¹ cm⁻¹)), 491 (6800), 570 (6100), 675^{sh} (500), 840 (44), 1875 (105).

trans-[OsBr₄{S(CH₂)₄}]₂ (**1c**). This was prepared similarly using *mer*-[OsBr₃{S(CH₂)₄}]₃ as starting material. Yield 65%. Anal. Calcd for C₈H₁₆S₂Br₄Os: C, 14.00; H, 2.35. Found: C, 13.9; H, 2.4. μ_{eff} (solid, 298 K): 1.71 μ_{B} . Spectral data: UV/visible/near-IR in CH₂Cl₂ (λ_{max} , nm (ϵ , M⁻¹ cm⁻¹)), 488 (8850), 550 (6350), 668 (440), 835 (38), 1810 (100).

mer-[OsBr₃(SMe₂)₃] (**2a**). This was prepared from (NH₄)₂[OsBr₆] and Me₂SO following the procedure described for **2b**.⁸ Yield: 30%. Anal. Calcd for C₆H₁₈S₃Br₃Os: C, 11.69; H, 2.94. Found: C, 11.8; H, 3.1. μ_{eff} (solid, 298 K): 1.89 μ_{B} . Spectral data: UV/visible/near-IR in CH₂Cl₂ (λ_{max} , nm (ϵ , M⁻¹ cm⁻¹)), 415 (5080), 460^{sh} (4450), 715 (60), 900^{sh} (28), 1540 (18). EPR in 1:1 CH₂Cl₂/toluene glass at 77 K (*g*₁, *g*₂, *g*₃), 2.79, 2.20, 1.72.

mer-[OsBr₃{S(CH₂)₄}]₃ (**2c**). This was prepared from (NH₄)₂[OsBr₆] and (CH₂)₄SO. Yield: 25%. Anal. Calcd for C₁₂H₂₄S₃Br₃Os: C, 20.75; H, 3.48. Found: C, 20.6; H, 3.6. μ_{eff} (solid, 298 K): 1.91 μ_{B} . Spectral data: UV/visible/near-IR in CH₂Cl₂ (λ_{max} , nm (ϵ , M⁻¹ cm⁻¹)), 415 (5000), 460^{sh} (2850), 717 (70), 930^{sh} (32), 1550 (24). EPR in 1:1 CH₂Cl₂/toluene glass at 77 K (*g*₁, *g*₂, *g*₃), 2.74, 2.23, 1.71.

X-ray Structure Determination. Single crystals of **1b** (0.11 × 0.20 × 0.21 mm³), **1c** (0.08 × 0.15 × 0.24 mm³), and **2c** (0.32 × 0.25 × 0.18 mm³) were grown by slow diffusion of hexane into the respective dichloromethane solutions. The cell parameters were determined by least-squares fits of 30 machine-centered reflections (2 θ , 14–28°). Data were collected at 295 K by ω -scan technique for **1b** (3 ≤ 2 θ ≤ 50°), **1c** (3 ≤ 2 θ ≤ 45°), and **2c** (3 ≤ 2 θ ≤ 45°), on a Nicolet R3m/V diffractometer with graphite-monochromated Mo K α radiation (λ = 0.710 73 Å). Two check reflections measured after every 98 reflections in each case showed no significant intensity reduction. Data were corrected for Lorentz–polarization effects. An empirical absorption correction based on ψ scan was applied in each case.¹³ The metal atoms were located from Patterson maps and the rest of the non-

Table 4. Crystallographic Data for **1b**, **1c**, and **2c**

	1b	1c	2c
chem formula	C ₂₈ H ₂₈ S ₂ Br ₄ Os	C ₈ H ₁₆ S ₂ Br ₄ Os	C ₁₂ H ₂₄ S ₃ Br ₃ Os
fw	938.5	686.2	694.4
space group	<i>P</i> 1̄	<i>P</i> 2 ₁ / <i>n</i>	<i>P</i> 2 ₁ / <i>c</i>
<i>a</i> , Å	6.792(3)	8.540(4)	7.278(2)
<i>b</i> , Å	9.931(4)	7.423(4)	19.228(4)
<i>c</i> , Å	11.792(5)	12.689(6)	13.791(4)
α , deg	97.70(3)		
β , deg	104.19(4)	108.94(4)	100.81(2)
γ , deg	98.88(3)		
<i>V</i> , Å ³	755.0(6)	760.9(6)	1896.0(11)
<i>Z</i>	1	2	4
<i>T</i> , °C	22	22	22
λ , Å	0.710 73	0.710 73	0.710 73
ρ_{calcd} , g cm ⁻³	2.085	3.002	2.439
μ , cm ⁻¹	97.66	191.74	134.02
<i>R</i> , %	5.47	6.46	4.45
<i>R</i> _w , %	6.00	7.49	5.32

^a $R = \sum ||F_o| - |F_c|| / \sum |F_o|$. ^b $R_w = [\sum w(|F_o| - |F_c|)^2 / \sum w|F_o|^2]^{1/2}$; $w^{-1} = \sigma^2(|F_o|) + g|F_c|^2$; $g = 0.0001, 0.001, \text{ and } 0.0005$ for **1b**, **1c**, and **2c**, respectively.

hydrogen atoms emerged from successive Fourier synthesis using $I > 3\sigma(I)$ as observed. The structures were refined by full-matrix least-squares procedures. All non-hydrogen atoms of **1b** and **1c** were refined anisotropically. In the case of **2c** all non-hydrogen atoms except C1, C2, C6, and C7 were refined anisotropically. The S(CH₂)₄ ring incorporating S1 displayed conformational disorder at C2. Hydrogen atoms were included in calculated positions with fixed $U = 0.08$ Å² in the final cycle of refinement. The highest difference Fourier peaks were 1.53, 1.64, and 1.21 e Å⁻³ (in the vicinity of Os) for **1b**, **1c**, and **2c** respectively. Significant crystal data are listed in Table 4. All calculations were done on a MICROVAX II computer using the SHELXTL-PLUS program package,¹⁴ and crystal structure plots were drawn using ORTEP.¹⁵

Acknowledgment. Financial support was received from Indian National Science Academy, Department of Science and Technology, and Council of Scientific and Industrial Research, New Delhi, are acknowledged. Affiliation with the Jawaharlal Nehru Centre for Advanced Scientific Research, Bangalore, India, is acknowledged.

Supporting Information Available: Tables of complete crystallographic data, atomic coordinates, bond distances and angles, anisotropic thermal parameters, and hydrogen atom positional parameters for **1b**, **1c**, and **2c** (16 pages). Ordering information is given on any current masthead page.

IC980142I

(14) Sheldrick, G. M. *SHELXTL-PLUS: Structure Determination Software Programs*; Siemens Analytical X-ray Instruments Inc.: Madison, WI, 1990.

(15) Johnson, C. K. *ORTEP*; Report ORNL-5138; Oak Ridge National Laboratory: Oak Ridge, TN, 1976.

(13) North, A. C. T.; Philips, D. C.; Mathews, F. S. *Acta Crystallogr.* **1968**, *A24*, 351.